Civil Engineering Infrastructures Journal xx,xx
DOI: 10.22059/CEIJ.2023.360871.1930

Influence of Variation of Soil Properties in Bearing Capacity and Settlement Analysis of a Strip Footing Using Random Finite Element Method

Vinay Kumar[1], Avijit Burman[2], F. H. M. Portelinha[1], Manish Kumar[3*] Guru Das[4]

[1] Department of Civil Engineering – DECiv, Universidade Federal de São Carlos - UFSCar, 235 Washington Luis Roadway, Mailbox 676, Zip Code: 13.565-905, Sao Carlos – SP, Brazil.

E-mail Address: kumarvinay@ufscar.br, ORCID iD: 0000-0001-7125-505X

E-mail Address: fportelinha@ufscar.br, ORCID iD: 0000-0002-7481-7406.

[2]Dept. of Civil Engineering, National Institute of Technology, Patna

E-mail Address: avijit@nitp.ac.in

[3]Department of Civil Engineering, SRM Institute of Science and technology (SRMIST) Tiruchirappalli,TN, 621105, India.

E-mail: mkumarod@gmail.com

[4]Dept. of Civil Engineering, National Institute of Technology, Patna

E-mail Address:gurud.ph21.ce@nitp.ac.in

* Corresponding author: Manish Kumar (E-mail: mkumarod@gmail.com)

Received: 21/06/2023
Revised: 03/10/2023
Accepted: 13/11/2023

ABSTRACT

This study analyzes bearing capacity and settlement for a strip footing at the proposed NIT Patna Bihta campus site. It uses the Random Finite Element Method (RFEM) based software, which combines viscoplastic finite element analysis with random field theory. The program generates random realizations of the soil domain using local average subdivision method. The average response of the soil domain with variable properties is estimated using Monte-Carlo simulation. The study assumes random variation of soil parameters like cohesion, friction angle, and elastic modulus, while Poisson's ratio and dilation angle are treated as deterministic variables. The study also considers the cross correlation between cohesion and friction angle. For no cross correlation, theoretical predictions are made for mean

and standard deviation of bearing capacity which are verified using Monte Carlo simulation based RFEM results. The probability of bearing capacity failure is also calculated using random finite element analysis and compared with theoretical results. The stochastic analysis of bearing capacity problem indicates that conservative results can be obtained with Prandtl's bearing capacity formula with consideration correlation length equal to the width of the footing. In settlement analysis, elastic settlement of strip footing on spatially variable soil is presented. Locally averaged lognormally distributed random fields of elastic modulus are generated to conduct probabilistic settlement analysis using RFEM, and it is seen that there is very good agreement between the predicted and the actual value of settlement at small and large correlation lengths. It is concluded that RFEM is a very suitable and efficient tool for investigation of the effect of variation of soil properties in determining the overall mean response for the bearing capacity and settlement behaviour.

Keywords: Bearing capacity analysis; settlement analysis; Mohr-Coulomb yield criteria; Random Finite Element Method; Monte Carlo Simulation.

1. INTRODUCTION

The foundation is the most important part of a structure as it connects the structure to the ground and transfers the load from the superstructure to the ground. In the literature, deterministic analysis is mostly used to calculate bearing capacity and settlement of foundation (Panwar & Dutta, 2023). Such analysis assumes the soil to have a uniform value of parameters like cohesion, friction angle, elastic modulus etc. But these values are not uniform over the soil domain. So, for an important structure, one needs to carry out the reliability analysis to find out the probability of failure and the associated risks. For such a purpose Fenton and Griffiths developed a program called Random Finite Element Method (RFEM) which is based on the combination of finite element method and random field theory. It has edge over the other reliability methods in the way that it can produce soil domains with spatially varying properties thus considering the uncertainty associated and hence the response of the soil domain to the loads will be more realistic. Many researchers have successfully been able to model this uncertainty using finite element method and other techniques (Halder & Chakraborty, 2022; Jimenez & Sitar, 2009; Johari & Talebi, 2021; D. R. Kumar et al., 2023; Mellah et al., 2000; Puła & Zaskórski, 2015; Rezaie Soufi et al., 2020; Q. L. Zhang & Peil, 1997). Viviescas et al., (2021) performed uncertainty quantification in the estimation of bearing capacity for shallow foundations in sandy soils using the finite element method. (Mofidi rouchi et al., 2014) perfprmed lower bound limit analysis for strip footings near slopes.

Griffiths and Fenton (2008) have used the program to carry out the probabilistic analysis of many geotechnical problems like flow problems, bearing capacity analysis, slope stability analysis etcetera. Fenton and Vanmarcke (1990) have developed a method called Local Average Subdivision (LAS) which have been popular for generating a realization of random field. Pieczyńska, Puła, Griffiths, & Fenton (2011) published their work on probabilistic analysis of bearing capacity including new factors, like introduction of anisotropy in the random fields of cohesion and friction angle. Another addition made in this study was that the soil was not considered weightless anymore. The inclusion of anisotropy produces more realistic results and effectiveness of RFEM predictions increases.

In recent years as well, many researchers have made use of this program to publish their work. Tan et al., (2009) performed slope stability analysis using fuzzy random finite element method. They said that fuzziness and randomness exist simultaneously in the soil and that is why it was important to carry out fuzzy random reliability analysis of slope. Pramanik et al., (2019) used fuzzy set theory along with RFEM to perform the reliability analysis of elastic settlement of surface strip footing resting on cohesionless soil. Johari et al., (2015) published their work for the case of loose sand. They carried out an analysis to find the reliability against static liquefaction. They used the RFEM for doing so. Monotonic loading was considered in their study. They employed a truncated normal probability density function to represent all the random parameters considered in the study. Rafael Jimenez and Nicholas Sitar (2009) performed RFEM analysis on foundation settlement. In their study they assumed different distributions for elastic modulus like lognormal, gamma and beta. They characterized the elastic modulus using random fields. The scale of fluctuation takes on the extreme values in their study. They performed their analysis for 2-dimensional shallow footing and the finite element model used was for plane strain condition. In recent years as well, a lot of research has been done on this topic (Q. L. Zhang & Peil, 1997). Wojciech Pula and Lukasz Zaskorski (2015) has published their work in which they investigated for a suitable distribution of the bearing capacity in case of cohesionless soil. In their study they assumed a bounded distribution for friction angle. The underlying Gaussian field was assumed to be tied with an ellipsoidal correlation function. They found that the probability distribution for the bearing capacity had a close resemblance with the Weibull distribution.

Luo and Bathurst (2018) carried out deterministic and random finite element analysis of unreinforced and reinforced embankments brought to failure using strip footing. Chenari et al., (2019) presented immediate settlement analysis of shallow foundation resting on a spatially random anisotropic soil layer. Chawla (2019) studied the worst case correlation length for mean bearing capacity values using RFEM. Selmi et al., (2019) performed capacity assessment of offshore skirted foundations subject to vertical horizontal moment loads using RFEM. Kawa and Pula (2020) carried out probabilistic bearing capacity analysis of footing on spatially variable soils in 3D using RFEM. Shu et al., (2020) studied the effect of autocorrelation distance on mean bearing capacity of Spudcan foundations. Ning and Zhe (2021) explored the effect of rotated anisotropy of soil property on the bearing capacity of embedded strip footings using RFEM. Arel and Mert (2021) dealt with settlement analysis of a vertically loaded strip footing using 2D RFEM. Kozlowska and Vessia (2022) calculated bearing capacity of shallow foundations considering drained and undrained condition using RFEM. He et al., (2023) compared the load and resistance factor design (LRFD) approach with the RFEM in case of shallow foundation in order to calibrate the LRFD based approach. D.K. et al., (2023) examined settlement of a strip footing placed on a two layered soil profile using random finite element model in conjunction with a hardening soil model. Hoek-Brown failure criterian was used to form stability charts (V. Kumar et al., 2023) Bendriss and Harichane (2023) performed seismic bearing capacity analysis of strip footing resting on soils having random soil properties and pseudo static seismic coefficient.

This study investigates influence of variation of soil properties in bearing capacity and settlement analysis of a strip footing in Bihta site where the construction of new campus of NIT Patna is proposed. The results of this study are obtained by using RFEM program (MRBEAR2D and MRSETL2D developed by Fenton and Griffith) (2008). To get the response of the system to applied loads, the program makes use of the finite element code. Also, the program

makes use of Monte Carlo simulation to estimate the probabilistic response a strip footing against bearing capacity failure of soil as well as the probability of failure against the settlement criteria. The paper describes the behavior of a strip footing for NIT Patna, Bihta campus for the first time, and this aspect can be regarded as a major contribution in the form of a case study of a real-life project.

2. METHODOLOGY

In this section, the concepts, terms, and the formulations that are used in this study will be introduced. As, in this study of bearing capacity and settlement analysis, soil of spatially varying properties is considered, the first step was to take observations from the site of our interest. After obtaining the raw data, a suitable distribution was decided upon for our variable. Then, a random field was defined and a realization was generated using random field generator. Evaluation of the response to this generated input should be done next. Generation of the realization and evaluation of the response was repeated for as many times as feasible. This whole process is called Monte Carlo simulation, i.e., producing possible replications of actual site conditions so that we can study the probabilistic nature of response.

2.1 Selection of a Distribution

In this study, the random process being considered is a continuous state and continuous space/time random process. Continuous state means that a variable can take any real value while continuous space/time means that the points, at which trials are done, are continuous in space or time. To represent continuous state processes, continuous probability distributions are used.

2.1.1 Normal Distribution

As per central limit theorem, when random variables are added together, they follow a normal distribution. Many natural phenomena in our surrounding are generally a sum of many random variables or involve many accumulating factors, and hence they tend to a normal distribution. A random variable P follows a normal distribution for the following form of pdf.

$$f(p) = \frac{1}{\sigma\sqrt{2\pi}} e^{\left[-\left(\frac{1}{2}\right)\left(\frac{p-\mu}{\sigma}\right)^2\right]} \quad \text{for } -\infty < p < \infty \tag{1}$$

A normal distribution can be completely represented by its mean (μ) and variance (σ^2). When multiple variables are involved, then also the mean and variance of each random variables can be used to show their behavior through normal distribution. The multivariate normal pdf has the following form:

$$f(p_1, p_2, \dots\dots, p_k) = \frac{1}{2\pi^{\frac{k}{2}}} * \frac{1}{|C|^{\frac{1}{2}}} * e^{\{-\frac{1}{2}(p-\mu)^T C^{-1}(p-\mu)\}} \tag{2}$$

Where $p_i's$ are the random variables, μ is the vector of mean values, one for each p_i, C is the covariance matrix between the $p_i's$ and |C| is its determinant. C is a $k \times k$ symmetric, positive definite matrix.

2.1.2 Lognormal Distribution

It is a non-negative distribution that can be obtained from normal distributions through simple transformation, If H is a normally distributed random variable, having range $-\infty < h < \infty$, then P = exp[H] will have a range $0 \leq p \leq \infty$. This random variable P will be lognormally distributed. Conversely, it can also be said that if ln (P) is normally distributed, then P will be lognormally distributed. So, if P is lognormally distributed random variable, it will have the probability density function

$$f(p) = \frac{1}{p\sigma_{lnP}\sqrt{2\pi}} e^{\left\{-\frac{1}{2}\left(\frac{ln\ p-\mu_{lnP}}{\sigma_{lnP}}\right)^2\right\}}, \qquad 0 \le p < \infty \tag{3}$$

where $\mu_{lnP} = E[ln\ P]$, ($E[ln\ P]$ represents expectation of P)

and $\sigma^2_{lnP} = Var\ [ln\ P]$

The mean and variance of $ln\ P$ can be found from mean and variance of P with the help of following relations

$$\sigma^2_{lnP} = ln\left(1 + \frac{\sigma_P^2}{\mu_P^2}\right) \tag{4}$$

$$\mu_{lnP} = ln\ (\mu_P) - \frac{1}{2}\sigma^2_{lnP} \tag{5}$$

2.1.3 Bounded Tanh Distribution

This distribution can also be derived from normal distribution using the following transformation

$$P = a + \frac{1}{2}(b-a)\left[1 + tanh\left(\frac{m+sG}{2\pi}\right)\right] \tag{6}$$

where, G is a normally distributed variable and X is bounded on the interval (a, b). The parameter 'm' is called location parameter. If m=0, then the distribution will be symmetric about midpoint. The parameter 's' is called scale parameter and it shows variability of the distribution. The pdf of P is

$$f_P(p) = \frac{\sqrt{\pi}(b-a)}{\sqrt{2}s(p-a)(b-p)} \times exp^{\left\{-\frac{1}{2s^2}\left[\pi ln\left(\frac{p-a}{p-b}\right) - m\right]^2\right\}} \tag{7}$$

In this study, cohesion and friction angles are treated as random variables with in bearing capacity analysis while elastic modulus will be our random variable in settlement analysis. But normal distribution has a shortcoming that it has non-zero probability of getting negative values. So, to overcome this problem, making use of lognormal distribution will be very helpful as it only yields positive values (Das et al., 2022) . Similarly, for elastic modulus, lognormal distribution will be an appropriate one. As friction angle is going to have both an upper bound and a lower bound, a bounded tanh distribution will be appropriate for it (Puła & Griffiths, 2021). Also, it resembles a beta distribution but obtained from transformation of a random field following normal distribution.

2.2 Defining a Random Field

In the present analysis, the random fields of the parameters involved in the determinations of bearing capacity and settlement of a shallow footing are created to conduct the necessary probabilistic analyses. The random fields used are continuous state-space in nature. Using the assumptions of random field being Gaussian and stationary, our requirements to characterize the field reduces to-

- Mean of the field, μ
- Variance of the field, σ
- Variation of the field in space

The last point can be captured by the covariance function (second moment of field's joint distribution).

2.3 Covariance Function and Correlation Function

It is already known that covariance measures how two variables change together. It is similar to variance for a joint probability distribution function. When more than one random variable is involved, it measures how two random variables changes with respect to each other. If P and Q random variables having joint probability distribution f_{PQ} (p, q), then the correlation for random variable P at positions x and x* can be expressed in terms of variances (i.e., σ_P and σ_Q) as well as the covariance matrix $C(x, x^*)$ in the following way:

$$\rho(x, x^*) = \frac{C(x, x^*)}{\sigma_P(x)\sigma_P(x^*)} \tag{8}$$

This helps in simplifying the probability models. Markov correlation function can be conveniently used in such cases with the following form:

$$\rho(\tau) = exp^{\{-\frac{2|\tau|}{\theta}\}} \tag{9}$$

where θ is the correlation length the length in the space domain up to which soil properties are significantly correlated. In this study, following correlation function is used for cohesion field

$$\rho_{lnc}(\tau) = e^{\{-\frac{2|\tau|}{\theta_{lnc}}\}} \tag{10}$$

The correlation length, θ_{lnc} is defined as the separation between two values of ln c that are significantly correlated and τ is the separation between two points for which correlation is being computed. A similar correlation function has been used for friction angle (ϕ) field. For elastic modulus field, following correlation function is used

$$\rho_{lnE}(\tau) = e^{\{-\frac{2|\tau|}{\theta_{lnE}}\}} \tag{11}$$

where θ_{lnE} is defined as the separation between two values of ln E that are significantly correlated. The cross correlation between c and ϕ are investigated at the correlation extremes (-1 and +1) as their correlation has no clear evidence in literature.

2.4 Variance Function

Most of the engineering properties are generally the local averages of some kind. Variance reduction function can be used to represent local averaging nature of any variable as

$$\gamma(X_1, X_2) = \frac{\theta_1^2\theta_2^2}{4X_1^2X_2^2}\left[\frac{2|X_1|}{\theta_1} + e^{\left\{-\frac{2|X_1|}{\theta_1}\right\}} - 1\right]\left[\frac{2|X_2|}{\theta_2} + e^{\left\{-\frac{2|X_2|}{\theta_2}\right\}} - 1\right] \tag{12}$$

where $X_1 \times X_2$ is the area of the plane for which local averaging is done. The Gaussian quadrature (numerical method) can also be used to compute the variance function instead of using Eq. (23), for more accurate results.

2.6 Generating a Realization of Random Field Using Local Average Subdivision (LAS) Method

This method of generating realization is fast and accurate, and therefore, has been adopted by many researchers in the past (Fenton & Griffiths, 2008). The majority of the measurements taken in the engineering field are actually the local averages of the property. That is why, using this method of generating realization can yield accurate results even for coarser meshes.

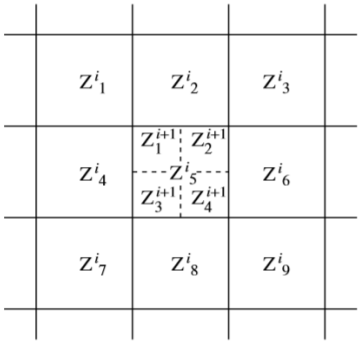

Fig. 1 Local average subdivision in 2 dimensions (Source: (Fenton & Griffiths, 2008))

As shown in Fig. 1, a normally distributed global average (Z_1^0) is generated with variance being same as derived in local averaging theory with zero mean. Next, the field is split up into four equal parts, and then four normally distributed values, Z_1^1, Z_2^1, Z_3^1 and Z_4^1 are generated in such a way that their mean and variances follows the below mentioned criteria:

(a) As per local averaging theory, the correct variance must be shown by them

(b) Proper correlation among them must be maintained

(c) Their average must be equal to the parent value, i.e. ¼ $(Z_1^1 + Z_2^1 + Z_3^1 + Z_4^1) = Z_1^0$

Then, each locally averaged cell thus obtained is again split up into four parts that must be equal, and the process is repeated. A 2D LAS algorithm for a sample function is shown in Fig. 2

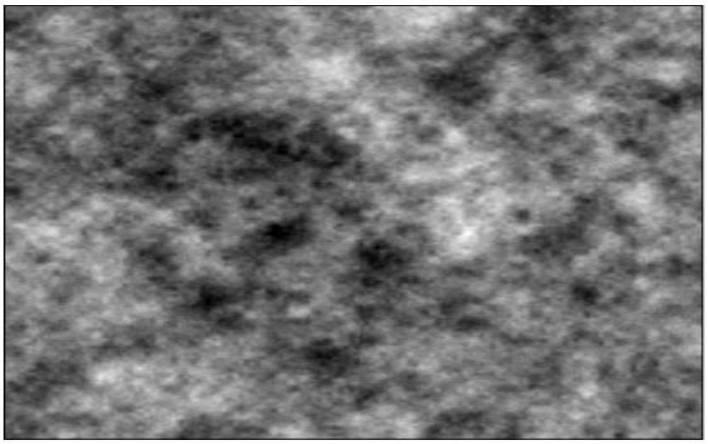

Fig. 2 2D sample function generated from LAS

2.6.2 Covariance Matrix Decomposition

It produces homogeneous random field through a simple direct method. However, it is only useful for small fields. A discrete process of zero mean $Z_i = Z(x_i)$, can be produced as per following formulation

$$Z = LU \tag{13}$$

where, L is a lower triangular matrix and satisfies the relationship $LL^T = C$ and U is a vector of n random variables of Gaussian nature. Each of them has zero mean and unit variance. C, in this case, represents a covariance matrix having elements $C_{ij} = C(\tau_{ij})$.

2.7 Methods Used in This Study

In this study, in bearing capacity analysis, cross correlation between the field of cohesion and the field of friction angle is implemented using covariance matrix decomposition. The random fields for cohesion, friction angle and elastic modulus are generated using LAS method. This process involves two steps. In the first step, the underlying Gaussian random field $G_{lnc}(x)$, $G_{\phi}(x)$ and $G_{lnE}(x)$, having zero mean, unit variance and Markov correlation function, are generated. Then using the following transformations, values of cohesion, c_i (i denotes the i^{th} element), friction angle, ϕ_i and elastic modulus E_i are obtained.

$$c_i = exp^{\{\mu_{lnc}+\sigma_{lnc}\times G_{lnc}(x_i)\}} \tag{14}$$

$$\phi_i = \phi_{min} + \frac{1}{2}(\phi_{max} - \phi_{min})\left\{1 + tanh\left(\frac{sG_{\phi}(x_i)}{2\pi}\right)\right\} \tag{15}$$

$$E_i = exp^{\{\mu_{lnE}+\sigma_{lnE}\times G_{lnE}(x_i)\}} \tag{16}$$

where x_i is the centroid of i^{th} element and $H(x_i)$ is the local average value generated by the LAS algorithm.

2.7.1 Finite Element Discretization of the Random Field Domain

In this study, the program by Fenton and Griffiths (2008) makes use of finite element method, which is a numerical method, is used for both bearing capacity and settlement problems, to obtain response of the system. In bearing capacity problem, footing is displaced until the failure happens while in settlement problem, a certain amount of load is placed on the footing and the settlement is recorded.

Governing Equations

Both the bearing capacity problem and settlement problem are represented using a 2D plane strain model. The governing equations for such a model are

$$\{\frac{\partial\sigma_x}{\partial x} + \frac{\partial\sigma_{xy}}{\partial y} + b_x = \frac{\rho\partial^2 u}{\partial t^2}\ \frac{\partial\sigma_{xy}}{\partial x} + \frac{\partial\sigma_y}{\partial y} + b_y = \rho\frac{\partial^2 v}{\partial t^2} \tag{17}$$

where normal stresses are represented by σ_x and σ_y, shear stress on planes xz and yz is represented by σ_{xy}, body forces per unit volume in x and y directions are represented by b_x and b_y respectively and displacements in x and y directions are represented by u and v respectively.

Boundary Conditions

In bearing capacity problem, eight-noded elements are used while in settlement problem, four-noded elements are used for discretizing the domain. The elements used are isoparametric elements i.e. they use same shape functions to define the element's geometric shape and the displacement within the element.

Boundary conditions have to be satisfied at a part of the boundary or the whole boundary, where a set of differential equations are to be solved. In bearing capacity problem, the left and right faces of the mesh can have translation in vertical direction but restricted against horizontal rotation. The bottom nodes are restricted against rotations as well as translation. Same boundary conditions apply in case of settlement problem.

In this study, for bearing capacity problem, the finite element mesh has 1000 elements. They are laid in such a way that width of the mesh occupies 50 elements while depth of the mesh occupies 20 elements. Each element has a dimension of 0.1m×0.1m. In settlement problem, the finite element mesh consists of 1200 elements. They are laid in such a way that width of the mesh occupies 60 elements and depth of the mesh occupies 20 elements. Each element has a dimension of 0.05m×0.05m. That makes the mesh 3 m wide and 1m deep.

2.7.2 Modelling of Soil as a Material

The stress-strain behaviour of soil under any general loading is essentially nonlinear. Therefore, it is necessary to consider a proper modelling technique to represent the nonlinear stress-strain behaviour of soil. In the present work, Mohr-Coulomb failure criterion is used to represent its constitutive behaviour of soil material. One of the popular methods for modelling material nonlinearity is to use 'constant stiffness' approach coupled with altering 'loads' vector as described by Smith et al., (2013). In such analysis, global stiffness matrix is only formed once and kept unchanged for rest of load application iterations. It is required to satisfy a properly defined yield criterion (in this case, Mohr-Coulomb failure criteria) to model the nonlinear stress-strain characteristic of the soil material. The 'loads' vector consists of externally applied loads as well as the self-equilibrating 'body loads'. The self-equilibrating 'body loads' vector is managed in such way so that the net loading on the system remains unchanged. The viscoplastic algorithm along with initial stress method is used by RBEAR2D and RSETL2D programs developed by Fenton and Griffiths (2008) to model the nonlinear stress-strain response of soil. These two programs have been used in the present study. Interested readers can find more information about the application of viscoplastic material nonlinearity for soil modelling in existing literatures (Zienkiewicz et al., 1969, 1977; Zienkiewicz & Cormeau, 1974).

2.7.3 Monte Carlo Simulations

Our objective to perform this simulation is to estimate the variance, mean and probabilities associated with response of system. To analyze the probability of the response of the system through Monte Carlo Simulation, it is required to carry out a significant number of simulations. For every simulation, a new realization of the random field is generated and response of the system is recorded.

In the bearing capacity analysis, 1000 simulations have been performed for probabilistic analysis. On the other hand, in case of settlement analysis, 5000 simulations have been performed for probabilistic analysis.

2.7.4 Formulations Used for Analysis of Results

Bearing Capacity

In literature, following relationship has been used frequently to determine bearing capacity

$$q_u = cN_c + \underline{q}N_q + \frac{1}{2}B\gamma N_\gamma \tag{18}$$

where q_u represents ultimate bearing stress, $\bar{q}$ represents overburden stress, c represents cohesion, γ represents unit weight of soil, N_c, N_q and N_γ represents bearing capacity factors and are the function of ϕ and B represents footing width. If we assume neglect the weight of the soil and that no surcharge is applied on the soil, then the above equation simplifies to

$$q_u = cN_c \tag{19}$$

This equation will be employed to get the statistics of bearing capacity. Up on dividing the equation by the cohesion mean, μ_c, it can be expressed in non-dimensionalized form as follows:

$$M_c = \frac{q_u}{\mu_c} = \frac{cN_c}{\mu_c} \tag{20}$$

where M_c is the bearing capacity factor and a stochastic equivalent of N_c. Now, it would become necessary to find the distribution of M_c. For that purpose, the distribution assumed for cohesion and friction angle, is lognormal distribution and bounded distribution respectively and their expressions are same as given in Eq. (14) and Eq. (15). In Eq. (21), geometric averages are employed for cohesion and friction angle, in order to present an approximate model.

$$M_c = \frac{\bar{c}\overline{N_c}}{\mu_c} \tag{21}$$

where $\overline{N_c} = \frac{e^{\pi tan\bar{\varphi}} tan^2\left(\frac{\pi}{4}+\frac{\bar{\varphi}}{2}\right)-1}{tan\bar{\varphi}}$

And $\bar{c}$ and $\bar{\phi}$ represents geometric averages of cohesion and friction angle. Using probability theory, following relations showing mean and variance of ln M_c can be found.

$$\mu_{lnM_c} \simeq lnN_c(\mu_\phi) - \frac{1}{2} ln\,(1 + \frac{\sigma_c^2}{\mu_c^2}) \tag{22}$$

$$\sigma^2_{lnM_c} \simeq \gamma(D)\{ln\left(1 + \frac{\sigma_c^2}{\mu_c^2}\right) + \left[\left(\frac{s}{4\pi}\right)(\phi_{max} - \phi_{min})\beta(\mu_\phi)\right]^2\} \tag{23}$$

Where γ(D) represents variance reduction function and ϕ is measured in radians. μ_c and μ_ϕ are the arithmetic mean of cohesion and friction angle fields

and $\beta(\phi) = \frac{bd}{bd^2-1}[\pi(1+a^2)d + 1 + d^2] - \frac{1+a^2}{a}$

here, $a = tan\,(\phi)\,, b = e^{\pi a}\ and\ d = tan\,(\frac{\pi}{4} + \frac{\phi}{2})$

All the other symbols have their usual meaning.

As the simulation results are in terms of bearing capacity, q_u, following results needs to be used to transform them in terms of bearing capacity factor, M_c. For number of realizations equal to 1000-

$$M_{c_i} = \frac{q_{u_i}}{\mu_c},\ \ i = 1,2,\ldots\ldots,1000 \tag{24}$$

$$\Rightarrow \quad \mu_{lnM_c} = \frac{1}{1000}\sum_{i=1}^{1000} lnM_{c_i}$$

$$\Rightarrow \quad \mu_{lnM_c} = \frac{1}{1000}\sum_{i=1}^{1000} ln\,(\frac{q_{u_i}}{\mu_c})$$

$$\Rightarrow \quad \mu_{lnM_c} = \mu_{lnq_u} - ln\mu_c \tag{25}$$

and

$$\sigma^2_{lnM_c} = \frac{1}{1000}\sum_{i=1}^{1000}(lnM_{c_i} - \mu_{lnM_c}) \tag{26}$$

$$\Rightarrow \quad \sigma^2_{lnM_c} = \frac{1}{1000}\sum_{i=1}^{1000}\left(ln\,\left(\frac{q_{u_i}}{\mu_c}\right) - (\mu_{lnq_u} - ln\mu_c)\right)^2$$

$$\Rightarrow \quad \sigma^2_{lnM_c} = \frac{1}{1000}\sum_{i=1}^{1000}(lnq_{u_i} - \mu_{lnq_u})^2$$

$$\Rightarrow \quad \sigma^2_{lnM_c} = \sigma_{lnq_u} \tag{27}$$

Settlement

Settlement problem is linear in many of its parameters. Elastic modulus is one of those parameters. So, a footing founded on a soil layer of uniform (but random) elastic modulus, E, can have the settlement, δ, of following form

$$\delta = \frac{\delta_{det}\mu_E}{E} \tag{28}$$

where δ_{det} is the deterministic value of settlement when $E = \mu_E$. Hence

$$\mu_{ln\delta} = ln\,(\delta_{det}) + ln\,(\mu_E) - \mu_{lnE}$$

$$\Rightarrow \quad \mu_{ln\delta} = ln\,(\delta_{det}) + \frac{1}{2}\sigma^2_{lnE} \tag{29}$$

and, as the local averaging is done, the standard deviation of log settlement is given by

$$\sigma_{ln\delta} = \sqrt{\gamma(B,H)}\sigma_{lnE} \tag{30}$$

where B×H is the averaging region on which variance reduction function, γ (B, H) depends.

2.7.5 Chi-Square Test

It is a goodness of fit test used for checking how much a hypothesized distribution fits the actual distribution. To do so, it performs a numerical comparison between predicted histogram and the observed one. Firstly, a histogram having k interval is constructed. Calculating the following value is the next step.

$$\chi^2 = \sum_{j=1}^{k}\frac{(N_j - np_j)^2}{np_j} \tag{31}$$

Where N_j is the number of observations in the j^{th} interval, n is the total number of observations and p_j is the probability that an observation lies in j^{th} interval in fitted distribution. The fitted distribution is rejected if

$$\chi^2 > \chi^2_{\alpha,k-1} \tag{32}$$

where α is the level of significance. The smallest value of α at which the fitted distribution is rejected is called p-value.

3. RESULTS AND DISCUSSIONS

3.1 General

In this section, the results of the study are presented and the efforts are made to explain a certain trend. These results of bearing capacity analysis and settlement analysis are for a strip footing founded on the Bihta site and are carried out by using MRBEAR2D and MRSETL2D part of RFEM software respectively, originally developed by Griffiths and Fenton (2008). The results are presented in two separate sections, one of which is dedicated to bearing capacity analysis while the other has the results of settlement analysis. In bearing capacity analysis, mean and standard deviation of log bearing capacity factor is plotted for various values of coefficient of variation, correlation length and cross correlation coefficient, and also a comparison has been made with the predicted values. In settlement analysis, mean and standard deviation of log settlement is plotted for various values of coefficient of variation, correlation length and cross correlation coefficient, and also a comparison has been made with the predicted values.

From the data obtained by exploration of Bihta site, on which new NIT Patna building is proposed, the averages for cohesion, friction angle and elastic modulus are calculated and are given below. In this study, the

probabilistic bearing capacity analysis and settlement analysis for a shallow footing is carried out, hence, while calculating averages, values of soil properties are considered for only up to 2.5 m depth.

$\mu_c \simeq 50\ kN/m^2$

$\mu_\phi = 5°$

$\mu_N = 15$

Som and Das (2003) recommended the use of the following empirical relationship to calculate elastic modulus E of soil based on SPT (N) value which was originally proposed by Schultz and Menzenbach (1961). Following relation between elastic modulus E and N value is used to calculate elastic modulus:

$E = 24 + 5.3N$

where E is in kg/cm^2. For the present analysis, following average value of elastic modulus (μ_E) is considered.

$\mu_E \simeq 10000\ kN/m^2$

3.2 Bearing Capacity Analysis

3.2.1 Input Data

In the bearing capacity analysis, a smooth rigid strip footing is considered which is assumed to be founded on weightless soil. Hence a plane stress condition prevailed. In this analysis a Mohr-Coulomb failure criterion is considered along with an elastic-perfectly plastic stress-strain law. A viscoplastic algorithm has been used to accomplish plastic stress redistribution. The finite element mesh consists of 50 elements wide by 20 elements deep i.e. 1000 elements. Eight noded quadrilateral elements are considered and each element has a size of 0.1m×0.1m. The strip footing is assumed to occupy 10 elements which makes its width equals to 1m.

Boundary Conditions

In bearing capacity problem, eight-noded elements are used while in settlement problem, four-noded elements are used for discretizing the domain. The elements used are isoparametric elements i.e. they use same shape functions to define the element's geometric shape and the displacement within the element.

Boundary conditions have to be satisfied at a part of the boundary or the whole boundary, where a set of differential equations are to be solved. In bearing capacity problem, the left and right faces of the mesh can have translation in vertical direction but restricted against horizontal rotation. The bottom nodes are restricted against rotations as well as translation. Same boundary conditions apply in case of settlement problem.

In this study, for bearing capacity problem, the finite element mesh has 1000 elements. They are laid in such a way that width of the mesh occupies 50 elements while depth of the mesh occupies 20 elements. Each element has a dimension of 0.1m×0.1m. Fig. 3 shows the geometry of the domain along with dimensions, and the support conditions.

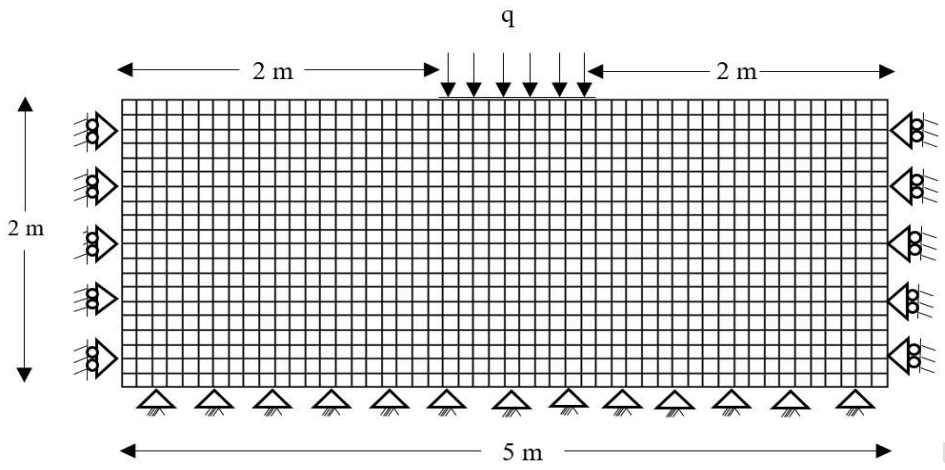

Fig. 3 Geometry of the domain and boundary conditions

Elastic modulus of soil, Poisson's ratio and dilation angle are assumed to be deterministic. Value of elastic modulus is set at 10000 kN/m^2 as obtained by averaging the field data. Poisson's ratio is set to 0.3 while dilation angle is assumed to be zero. The cohesion and friction angle are set as random parameters. A lognormal distribution is assumed to characterize cohesion while a bounded tanh distribution is assumed to characterize friction angle. Local average subdivision method is used to generate random fields of cohesion and friction angle. Covariance matrix decomposition method is used to establish cross correlation between cohesion and friction angle. The scale factor of friction angle is set equal to coefficient of variation of cohesion. The mean of cohesion is set to 50 kN/m^2 as obtained by averaging. The mean of friction angle is set at 5° as obtained by averaging. The upper bound for friction angle is set at 9° and lower bound is set at 1°. Fig. 4 and 5 show the cohesion and friction angle random fields for the 'ith' simulation.

Varying values of correlation length, coefficient of variation and cross correlation coefficient are used in this study. Monte Carlo simulations involving 1000 realizations are performed. Each realization has a different soil property random field and hence a different bearing capacity value.

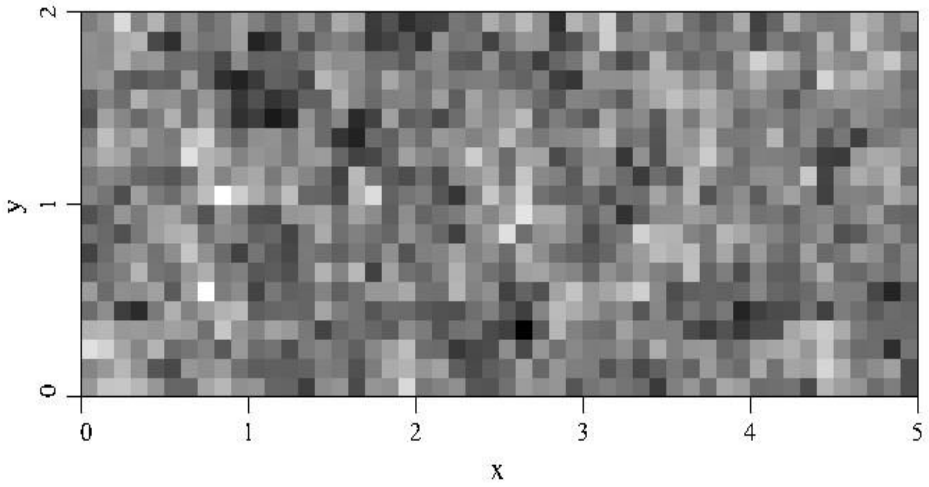

Fig. 4 Cohesion random field

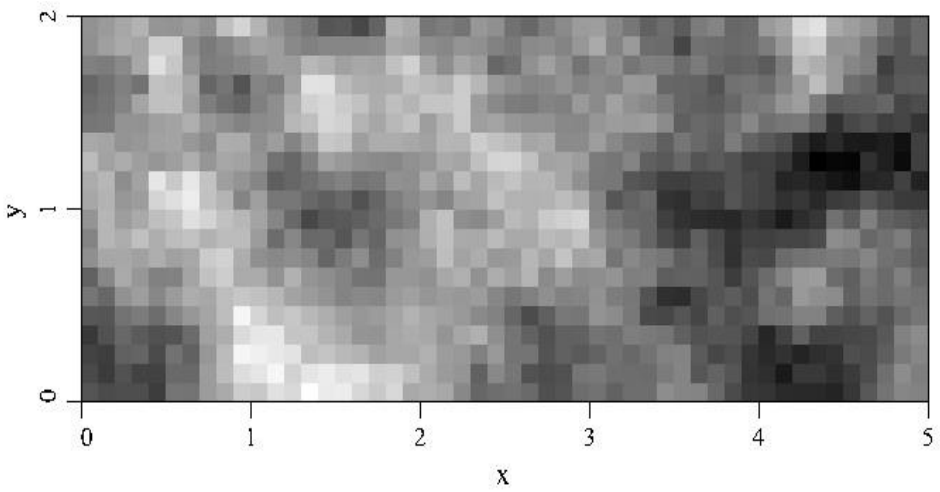

Fig. 5 Friction angle random field

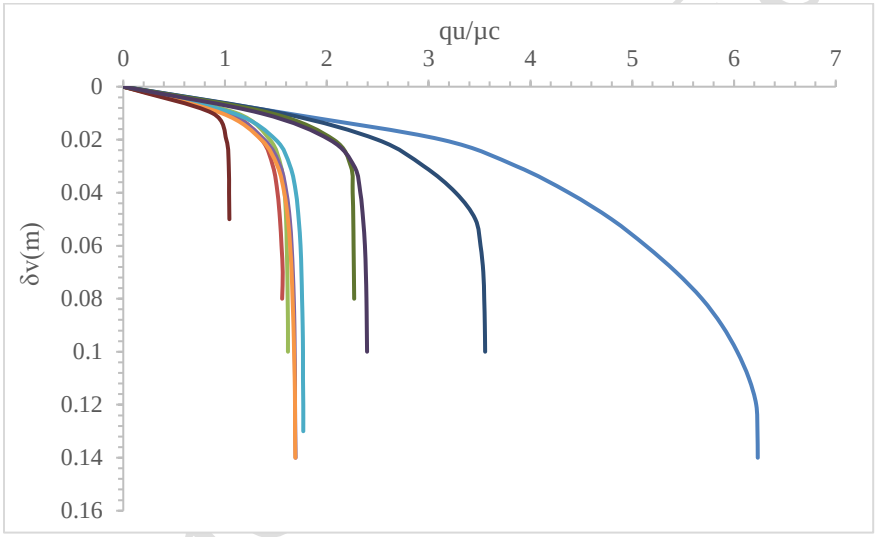

Fig. 6 Load-deformation curves corresponding to different realizations of soil

In Fig. 6, q_u is the bearing capacity, μ_c is the mean value of cohesion and δ_v represents the deformation in the soil. The stress-strain and load-displacement response of soil is nonlinear. Calculation of bearing capacity and settlement. Fig. 7 shows a deformed finite element mesh at failure for a soil having spatially random properties.

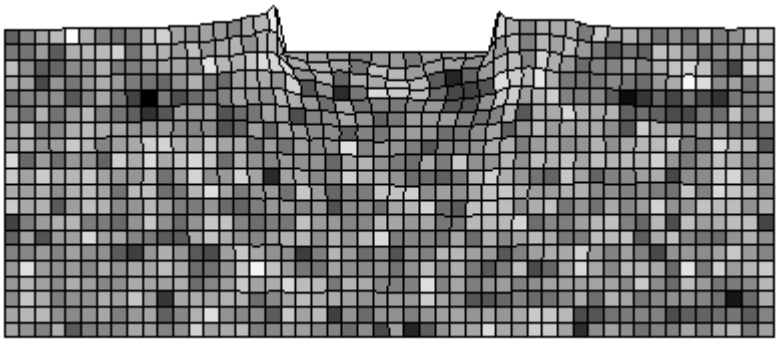

Fig. 7 Deformed finite element mesh at failure of soil having random properties, lighter regions indicate weaker soil

It can be seen that the failure surface is not strictly logarithmic spiral. The reason for the deviation could be that the path followed by the failure surface is through the weakest soil regions which might not be strictly logarithmic spiral in case of spatially variable soil. This deviation indicates that considering the randomness of soil while calculating bearing capacity is important to avoid overestimation or underestimation of N factors (which are calculated by assuming the failure surface to be log-spiral in most cases).

3.2.2 Mean of Log Bearing Capacity Factor vs. Cohesion

In our study, efforts are made to find out the variation of mean of log bearing capacity factor (μ_{lnMc}) with coefficient of variation, correlation length and cross correlation coefficient. A comparison has also been made with the predicted mean as per Eq. (22). Also, as the results of simulation were obtained in terms of bearing capacity, to convert them in terms of log bearing capacity factor, Eq. (25) is used. Results are presented below in graphical form. ρ represents the cross-correlation coefficient while θ represents correlation length.

As predicted by Eq. (22), the value of μ_{lnMc} tends towards deterministic value ln $N_c(\mu_\phi)$ i.e. 1.87008 when variability of soil is small and mean properties are taken everywhere. Several researchers (Haldar & Mahadevan, 2000); (Der Kiureghian & Ke, 1988)(Johari et al., 2015) have suggested different choices of the correlation length for use in a RFEM simulation. A ratio varying between 4 and 8 for the correlation length to the length of finite element was suggested by Der Kiureghian and Ke (1988). However, Fenton and Griffiths (2008) considered correlation length as high as 8 for a similar sized footing considered in the present study, while investigating bearing capacity problem using RFEM. In this analysis, the correlation length has been varied from 0.1 m to 1.0 m. The minimum correlation length is considered equal to the size of the element used, whereas the maximum correlation length is considered as equal to the size of the footing i.e., 1.0 m. However, following the works of Fenton and Griffith (2008), the influence of correlation length C.L = 8 is also studied. The variation of μ_{lnMc} vs. dimensionless parameter σ_c/μ_c is shown in Fig. 8. As the variability increases, a significant reduction from the Prandtl's solution can be observed. Soils having perfect correlation between cohesion and friction angle appear to be most affected while the least reduction has been observed in negatively correlated soils. The independent case lies between the two. By some authors in the literature, it has been cited that cohesion and friction angle are negatively correlated. So, if the soil parameters are assumed to be uncorrelated while designing, then that will yield results on the conservative side.

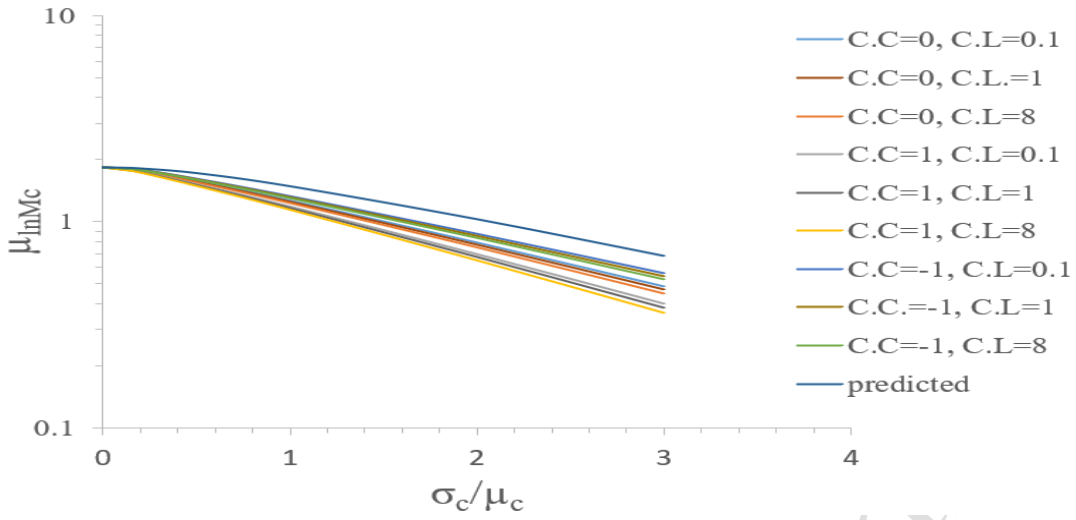

Fig. 8 Sample mean of lnM_c along with the predicted one

The effect of θ does not appear too much, but still the values are lower than the predicted ones. Also, Eq. (22) does not incorporate the effect of correlation length. Hence a separate plot is presented in section 3.2.4 to analyze the effect of correlation length.

3.2.3 Standard Deviation of Log Bearing Capacity Factor vs. Coefficient of Variation of Soil

Results for standard deviation of log bearing capacity factor are presented below as a graphical plot in Fig. 9. From the above results it is evident that cross-correlation coefficient does not have significant effect on standard deviation of log bearing capacity factor. However, the correlation length does affect it quite significantly. The variation reduction function decreases with decrease in correlation length. Also, from Eq. (23), it is clear that standard deviation of log bearing capacity factor depends upon variance reduction function. Hence, with decrease in correlation length, the standard deviation of log bearing capacity factor decreases.

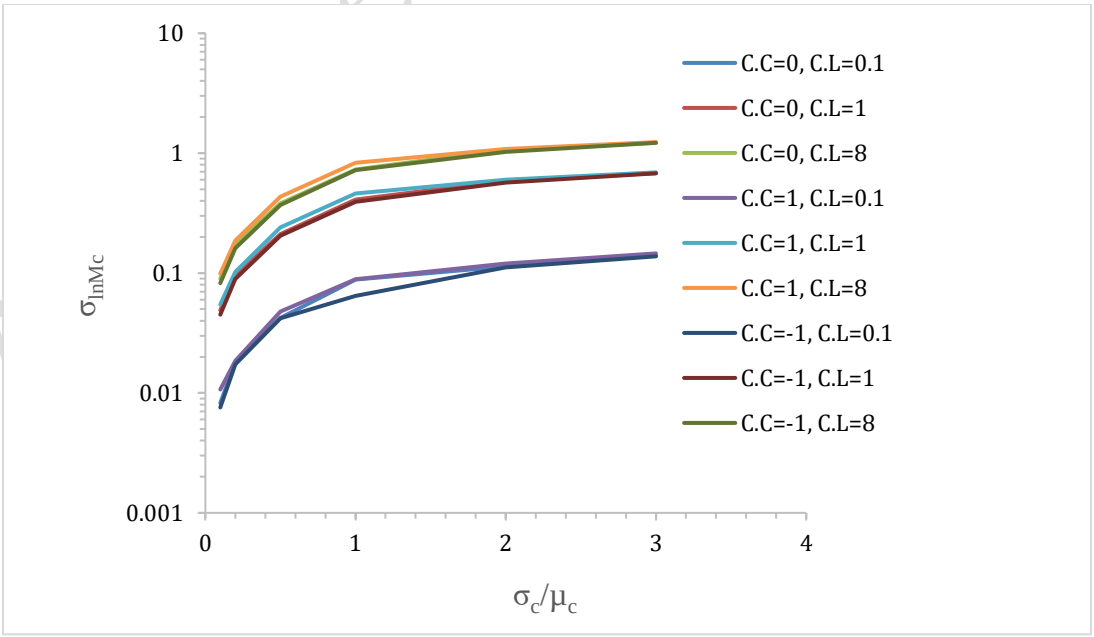

Fig. 9 Sample standard deviation of ln M_c

3.2.4 Sample Mean of Log Bearing Capacity Factor vs. Correlation Length

The results presented in this section show how the sample mean of log bearing capacity factor varies with correlation length. The results of the simulation are presented below as a graphical plot (Fig. 10). When correlation length tends towards infinity, the mean value of log bearing capacity factor tends towards the value as predicted by Eq. (22). An effort can be made to explain the reasoning behind this. When correlation length tends towards infinity, the soil properties becomes spatially constant for a particular realization. Hence the failure surface returns to log spiral and mean values tends towards the predicted ones. Also, it is evident from the graph that when correlation length tends towards zero (i.e. infinitely rough field), the mean values approaches the predicted ones. In this case, the weakest path becomes very long and failure surface has to return to log spiral.

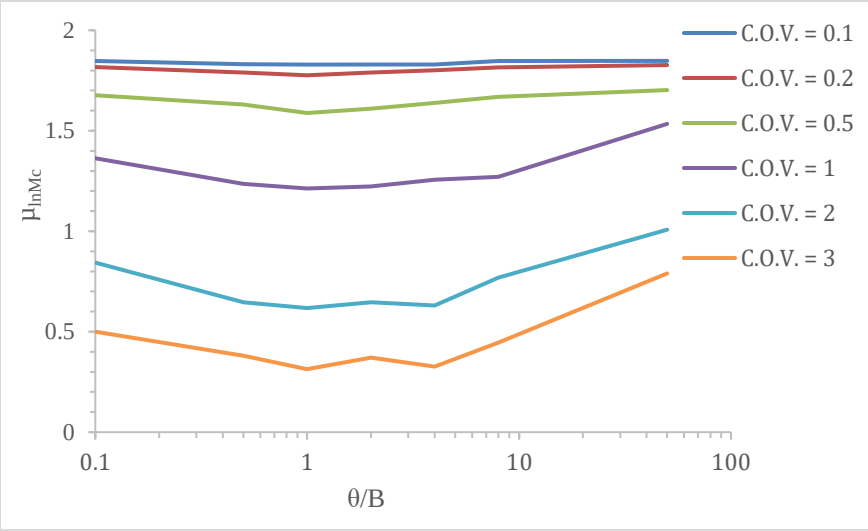

Fig. 10 A plot of sample μ_{lnMc} versus normalized correlation length (θ/B)

From Fig. 10, it is clear that for different values of coefficient of variation, the mean of log bearing capacity factor is minimum when correlation length and width of footing are of same order. As the correlation lengths 0.1 and 8 are approximately equally spaced from θ = 1, hence their plots lie so close.

3.2.5 Sample Mean of Log Bearing Capacity Factor vs. Coefficient of Variation

As observed in the previous plot, when correlation length and width of footing are of same order, the sample mean of log bearing capacity factor deviates most from the value predicted in Eq. (22). Hence the Eq. (22) needs to be modified to give conservative results. Also, the equation is modified in a way to give conservative results for worst correlation length for a zero value of cross correlation coefficient. Weakest path issue and a slight finite element model error are the reasons that such a correction is needed. The modified equation with empirical correction is

$$\mu_{lnM_c} \simeq 0.92 lnN_c(\mu_\phi) - 0.7 ln\,(1 + \frac{\sigma_c^2}{\mu_c^2}) \tag{33}$$

Fig. 11 shows the plot for μ_{lnMc} for different values of coefficient of variation and θ, is for ρ=0.

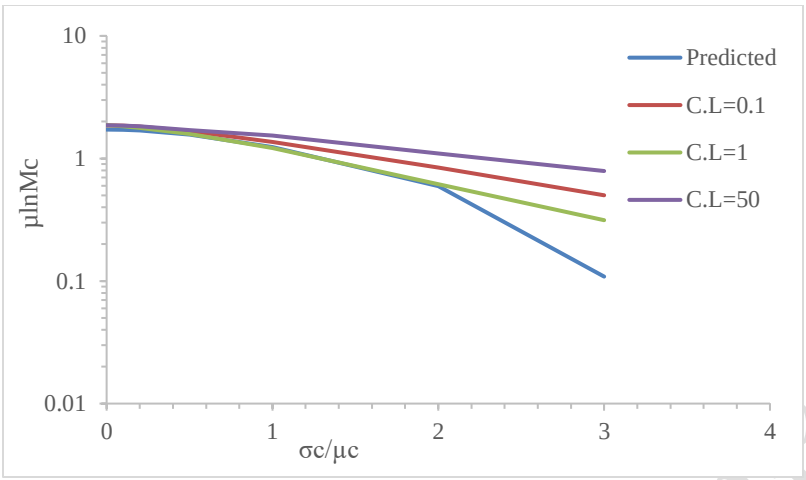

Fig. 11 Plot of Sample and estimated mean of ln M_c versus ν, for different θ

3.2.6 Sample Standard Deviation of Log Bearing Capacity Factor vs. Coefficient of Variation

In this section, a comparison is done between the sample standard deviation and the ones predicted from Eq. (23). The domain size required to calculate the variance reduction function is taken as a region having mean wedge zone depth, w and width of 5w, where w is

$$w \simeq \frac{1}{2} B tan\left(\frac{1}{4}\pi + \frac{1}{2}\mu_{\phi}\right) \tag{34}$$

Hence γ(D) becomes equal to γ (5w, w). This domain D approximately gives the area involved in failure region. It represents the area between mean log spiral curves on both sides of footing. The results of the simulation along with the predicted ones are given as a graphical plot in Fig. 12. They are for a cross-correlation coefficient equals to zero. A close agreement between simulated values and predicted values can easily be seen. The variability involved in the weakest path and the variability involved in any nearby path in a statistically homogeneous medium will be similar and hence, this close agreement.

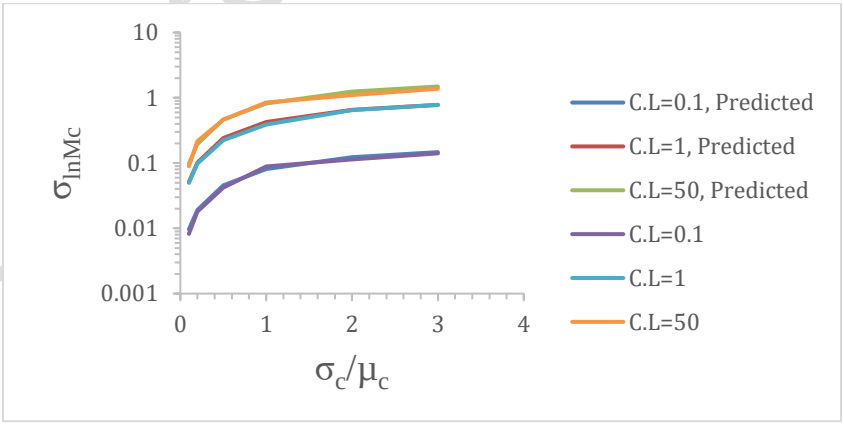

Fig. 12 Plot of sample and estimated standard deviation of ln M_c versus ν, for different θ

3.2.7 Estimation of Probability Density Function of Bearing Capacity

An estimation of probability density function of bearing capacity is done through Monte Carlo simulations and goodness of fit analysis is performed through chi square test. This test yields a value called p-value. If p-value is

high, then goodness of fit is high and vice versa. This test was performed for all the results and an average p value of 30 percent was obtained, which is high enough for good agreement with hypothesized distribution. Few percentage of simulations have p-value less than 5 percent. Around 10 percent of simulations has p-value less than 0.01 percent. Fig. 13 (a) Fig. 13 (b) show two fits with different values of coefficient of variation and correlation length. Even with the smaller p-values, a reasonable fit can be seen. Hence it can be said that bearing capacity approximately follows lognormal distribution.

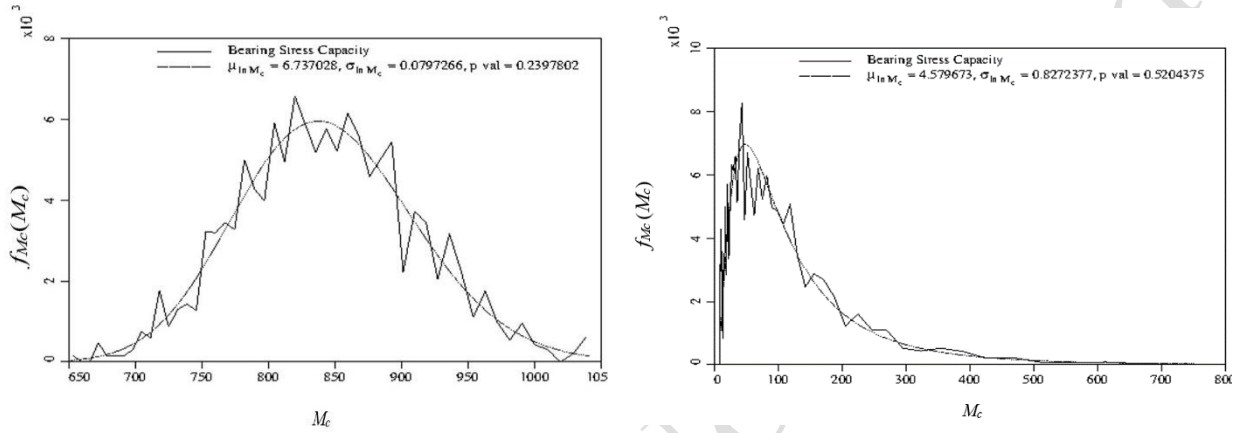

(a) (b)

Fig. 13 (a) Fitted lognormal distribution for $s=\sigma_c/\mu_c=0.1$, $\theta=4$ and $\rho=0$ having large p-value and (b) fitted lognormal distribution for $s=\sigma_c/\mu_c=5$, $\theta=1$ and $\rho=0$ having small p-value

3.3 Settlement Analysis

3.3.1 Input Data

Two dimensional settlement analysis is done for single footing. Elastic theory is used to calculate both the immediate settlement and consolidation settlement (Terzaghi Karl, 1943). The soil on which footing is founded, is assumed to be underlain by bedrock. A 2D plane strain model is used to represent the physical problem.

The finite element mesh consists of four noded quadrilateral elements. Each element is a square of side 0.05m. The mesh has 100 elements in the horizontal direction and 40 elements in the vertical direction. This makes the width of the mesh equals to 5m and depth of the mesh equals to 2m. A fixed load of 1000 kN is applied to the footing. Value of Poisson's ratio was fixed at 0.25. Mean value of elastic modulus is fixed at 10000kN/m^2. Elastic modulus was assumed to follow lognormal distribution and its random field was generated using local average subdivision method. Standard deviation of elastic modulus, width of footing and correlation length are varied. Monte Carlo simulations were used and for each input parameter, 5000 realizations were performed. An RFEM representation of single footing is given below in Fig. 14.

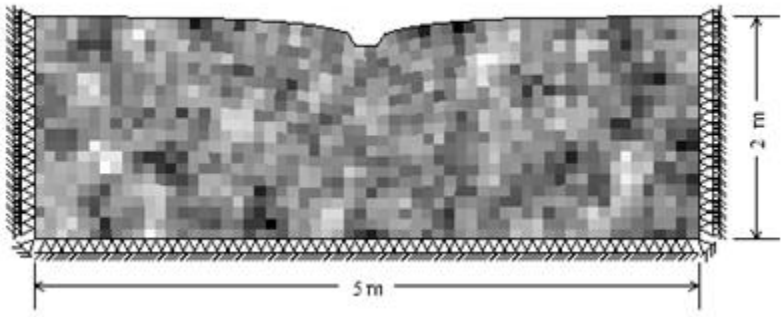

Fig. 14 RFEM representation of single footing

3.3.2 Mean of Log Settlement vs. Variance of Log Elastic Modulus

The results for variation of mean of log settlement ($m_{ln\delta}$) with respect to variance of log elastic modulus (σ^2_{lnE}) for different values of correlation length are presented below as a graphical plot in Fig. 15 to show the variation. These results are for a footing of width 0.1m.

All the correlation length is plotted in the figure but they are not identifiable because they lie very close to each other. This shows that mean of log settlement does not depends very much on the correlation length. As mean of the local averaging process is not affected by correlation length, hence this shouldn't be a surprise. Also, the simulation results show good agreement with the results predicted by Eq. (29).

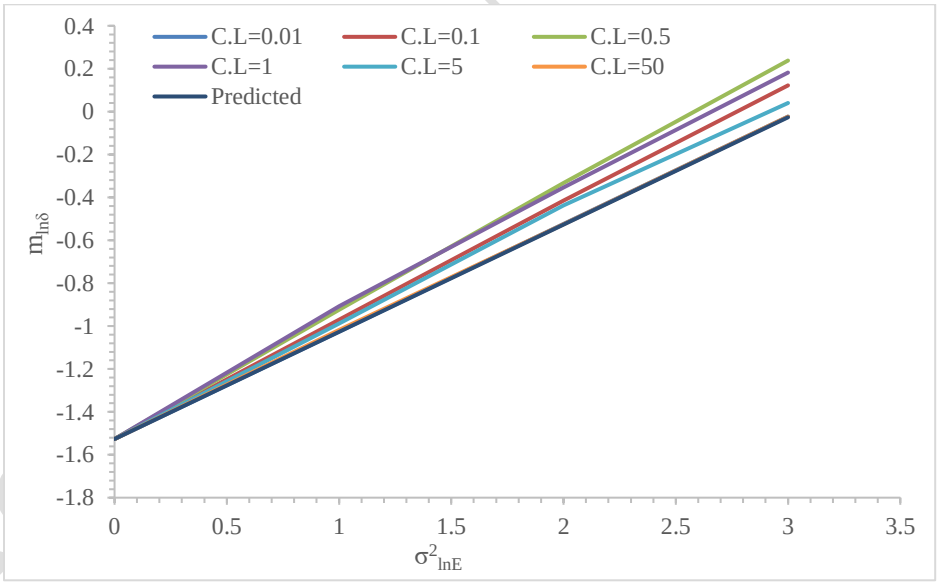

Fig. 15 Estimated mean of log settlement along with the predicted ones

3.3.3 Standard Deviation of Log Settlement vs. Correlation Length for Different Footing Width

The results for simulated standard deviation of log settlement ($s_{ln\delta}$) for different values of correlation length, footing width and coefficient of variation of elastic modulus are shown below as a graphical plot in Fig. 16 for comparison between simulated results and results predicted from Eq. (30).

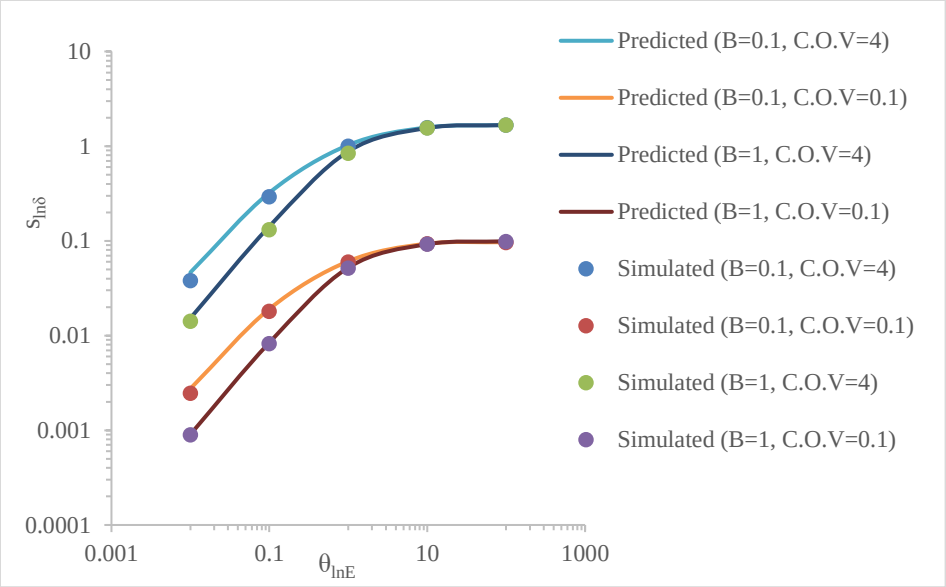

Fig. 16 Comparison of simulated and theoretical standard deviation of log settlement

As correlation length tends to zero, the values of elastic modulus at any two distinct points becomes independent. Therefore, with decrease in correlation length, the value of variance function decreases. In other words, due to local averaging process, the values of elastic modulus tend towards mean value. Hence, from Eq. (30) we can say that the standard deviation of log settlement tends towards zero with the mean value approaching deterministic value. While for another limiting case, when correlation length approaches infinity, the elastic modulus field becomes uniform but still random from realization to realization. Variance reduction function for such a field will approach to unity. So basically, the plot is actually showing the variation of variance reduction function with respect to the correlation length. The agreement between simulated results and predicted results is quite remarkable at small and large correlations lengths and for intermediate correlation lengths also, the agreement is good.

3.3.4 Probability Density Function of Settlement

A histogram of the settlement is shown in following Fig. 17. This is a normalized histogram as the frequency density plot was desired. Parameters used to produce this histogram are- B=0.1m, ν=1 and θ=0.1. A lognormal distribution is superimposed on it.

In appearance, the lognormal distribution seems quite fit. But this simulation had one of the least p-value of chi square test. For other simulations p-value was not this low. Hence it would be safe to say that settlement follows the lognormal distribution.

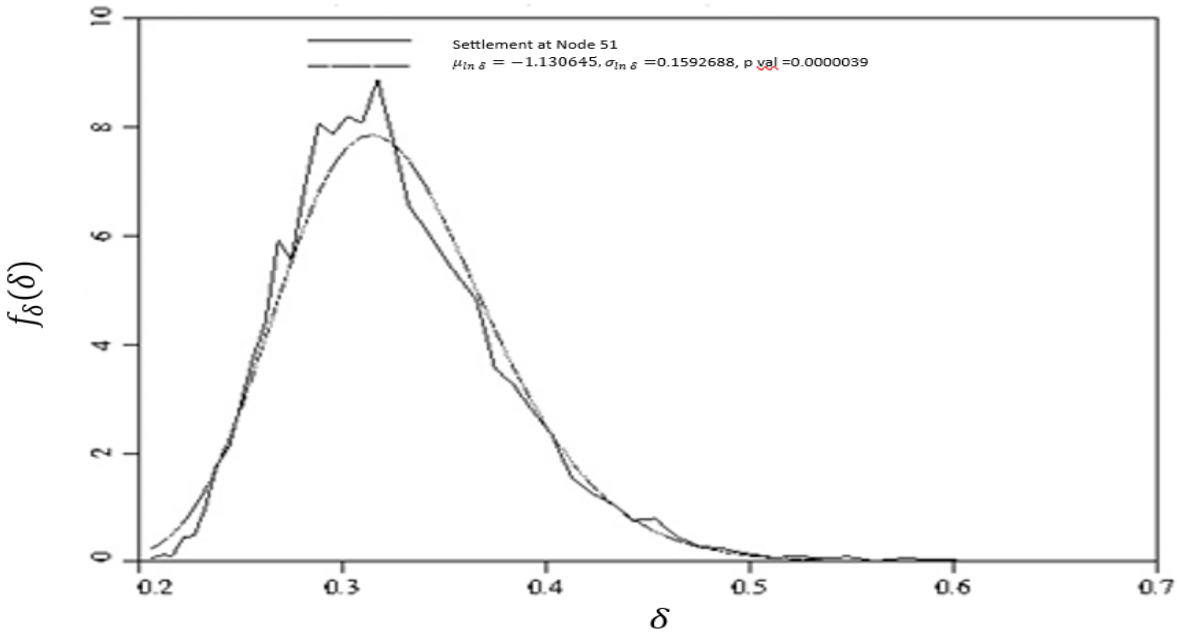

Fig. 17 Frequency density plot of settlement and fitted lognormal distribution

4. CONCLUSIONS

This study of the effect of variation of soil properties on baring capacity analysis of a strip footing founded in NIT Patna Bihta campus concludes that on average, the bearing capacity of a soil having spatially varying properties will be less than the bearing capacity calculated from Prandtl's formula using only mean values. When the soil properties become random in nature, the failure surface shifts from logarithmic spiral to a surface which is weaker and exists in the vicinity of the spiral one. To predict the statistics of bearing capacity, it is possible to use Prandtl's formula if the geometric averages are the basis for the properties used in the formula. Although an empirical adjustment is needed for mean. The stochastic behavior of bearing capacity does not seem to be much affected by cross correlation between cohesion and friction angle. Anyway, the independent case was found to be conservative. Generally, the information about correlation length at a site is not available. For such instances a worst case correlation length ($\theta \simeq B$) was found. So if the design is based on this correlation length, it would be conservative.

The settlement study concludes that lognormal distribution appropriately represents the settlement of the footing placed on the soil having spatially random elastic modulus represented by lognormal distribution itself. Mean along with the variance of the log elastic modulus field are the parameters that are required to represent mean of log settlement. Using the limiting values of correlation length, it is possible to approximate the mean of log settlement. When log elastic modulus field is locally averaged directly under the footing and its variance is taken, it will produce the quantity that very accurately approximates the standard deviation of log settlement.

Author`s Contributions:

V. Kumar: Analysis and manuscript writing; A. Burman: Conceptualization, checking results, and manuscript finalization. F. H. M. Portelinha: Checking results, review, editing, and manuscript finalization; Utkarsh Mishra: Analysis, checking results, review, editing, and manuscript finalization; Manish Kumar: Checking results, review, editing, and manuscript finalization.

Declarations

Funding

The research is partially funded by the Ministry of Science and Higher Education of the Russian Federation under the strategic academic leadership program 'Priority 2030' (Agreement 075-15-2021-1333 dated 30 September 2021).

Conflicts of interest/Competing interests

The submitted work does not have pose any conflict of interest/competing interests with anyone else's works.

REFERENCES

Arel, E., & Mert, A. C. (2021). Field simulation of settlement analysis for shallow foundation using cone penetration data. *Probabilistic Engineering Mechanics*, *66*, 103169. https://doi.org/10.1016/j.probengmech.2021.103169

Bendriss, F., & Harichane, Z. (2023). Reliability-based analysis of seismic bearing capacity of shallow strip footings resting on soils with randomly varying geotechnical and earthquake parameters. *Soils and Rocks*, *47*, e2024078821.

Chwała, M. (2019). Undrained bearing capacity of spatially random soil for rectangular footings. *Soils and Foundations*, *59*(5), 1508–1521. https://doi.org/10.1016/j.sandf.2019.07.005

Das, G., Burman, A., Bardhan, A., Kumar, S., Choudhary, S. S., & Samui, P. (2022). Risk estimation of soil slope stability problems. *Arabian Journal of Geosciences*, *15*(2), 204. https://doi.org/10.1007/s12517-022-09528-y

Der Kiureghian, A., & Ke, J. Bin. (1988). The stochastic finite element method in structural reliability. *Probabilistic Engineering Mechanics*, *3*(2), 83–91. https://doi.org/10.1016/0266-8920(88)90019-7

D.K., T., M., C., & W., P. (2023). Probabilistic Foundation Settlement using A Hardening Soil Model on Layered and Spatially Variable Soil. In *Geo-Risk 2023* (pp. 447–453). https://doi.org/10.3850/978-981-18-5184-1_ms-13-189-cd

Fenton, G. A., & Griffiths, D. V. (2008). Risk Assessment in Geotechnical Engineering. In *Risk Assessment in Geotechnical Engineering* (Vol. 461). John Wiley & Sons New York. https://doi.org/10.1002/9780470284704

Fenton, G. A., & Vanmarcke, E. H. (1990). Simulation of Random Fields via Local Average Subdivision. *Journal of Engineering Mechanics*, *116*(8), 1733–1749. https://doi.org/10.1061/(asce)0733-9399(1990)116:8(1733)

Haldar, A., & Mahadevan, S. (2000). *Reliability assessment using stochastic finite element analysis*. John Wiley & Sons.

Halder, K., & Chakraborty, D. (2022). Probabilistic response of strip footing on reinforced soil slope. *Risk, Reliability and Sustainable Remediation in the Field of Civil and Environmental Engineering*, *116*, 333–358. https://doi.org/10.1016/B978-0-323-85698-0.00021-6

He, P., Fenton, G. A., & Griffiths, D. V. (2023). Load and resistance factor design versus reliability-based design of shallow foundations. *Georisk*, *17*(2), 277–286. https://doi.org/10.1080/17499518.2022.2083179

Jamshidi Chenari, R., Pourvahedi Roshandeh, S., & Payan, M. (2019). Stochastic analysis of foundation immediate settlement on heterogeneous spatially random soil considering mechanical anisotropy. *SN Applied Sciences*, *1*(7), 1–15. https://doi.org/10.1007/s42452-019-0684-0

Jimenez, R., & Sitar, N. (2009). The importance of distribution types on finite element analyses of foundation settlement. *Computers and Geotechnics*, *36*(3), 474–483. https://doi.org/10.1016/j.compgeo.2008.05.003

Johari, A., Pour, J. R., & Javadi, A. (2015). Reliability analysis of static liquefaction of loose sand using the random finite element method. *Engineering Computations*.

Johari, A., & Talebi, A. (2021). Stochastic Analysis of Piled-Raft Foundations Using the Random Finite-Element Method. *International Journal of Geomechanics*, *21*(4), 4021020. https://doi.org/10.1061/(asce)gm.1943-5622.0001966

Kawa, M., & Puła, W. (2020). 3D bearing capacity probabilistic analyses of footings on spatially variable c–φ soil. *Acta Geotechnica*, *15*(6), 1453–1466. https://doi.org/10.1007/s11440-019-00853-3

Kumar, D. R., Samui, P., Wipulanusat, W., Keawsawasvong, S., Sangjinda, K., & Jitchaijaroen, W. (2023). Soft-Computing Techniques for Predicting Seismic Bearing Capacity of Strip Footings in Slopes. *Buildings*, *13*(6), 1371. https://doi.org/10.3390/buildings13061371

Kumar, V., Burman, A., & Kumar, M. (2023). Generic form of stability charts using slide software for rock slopes based on the Hoek–Brown failure criterion. *Multiscale and Multidisciplinary Modeling, Experiments and Design*, 1–15. https://doi.org/10.1007/S41939-023-00265-7/METRICS

Luo, N., & Bathurst, R. J. (2018). Deterministic and random FEM analysis of full-scale unreinforced and reinforced embankments. *Geosynthetics International*, *25*(2), 164–179. https://doi.org/10.1680/jgein.17.00040

Luo, N., & Luo, Z. (2021). Reliability Analysis of Embedded Strip Footings in Rotated Anisotropic Random Fields. *Computers and Geotechnics*, *138*, 104338. https://doi.org/10.1016/j.compgeo.2021.104338

Mellah, R., Auvinet, G., & Masrouri, F. (2000). Stochastic finite element method applied to non-linear analysis of embankments. *Probabilistic Engineering Mechanics*, *15*(3), 251–259. https://doi.org/10.1016/S0266-8920(99)00024-7

Mofidi rouchi, J., Farzaneh, O., & Askari, F. (2014). Bearing Capacity of Strip Footings near Slopes Using Lower Bound Limit Analysis. *Civil Engineering Infrastructures Journal*, *47*(1), 89–109. https://doi.org/10.7508/ceij.2014.01.007

Panwar, V., & Dutta, R. K. (2023). Development of Bearing Capacity Equation for Rectangular Footing under Inclined Loading on Layered Sand. *Civil Engineering Infrastructures Journal*, *56*(1), 173–192. https://doi.org/10.22059/CEIJ.2022.339138.1819

Pieczyńska, J., Puła, W., Griffiths, D. V, & Fenton, G. A. (2011). Probabilistic characteristics of strip footing bearing capacity evaluated by random finite element method. *Proceedings of the 11th International Conference on Applications of Statistics and Probability in Soil and Structural Engineering (ICASP), Zurich*, *10*.

Pieczyńska-Kozłowska, J., & Vessia, G. (2022). Spatially variable soils affecting geotechnical strip foundation design. *Journal of Rock Mechanics and Geotechnical Engineering*, *14*(3), 886–895. https://doi.org/10.1016/j.jrmge.2021.10.010

Pramanik, R., Baidya, D. K., & Dhang, N. (2019). Implementation of Fuzzy Reliability Analysis for Elastic Settlement of Strip Footing on Sand Considering Spatial Variability. *International Journal of Geomechanics*, *19*(12), 4019126. https://doi.org/10.1061/(asce)gm.1943-5622.0001514

Puła, W., & Griffiths, D. V. (2021). Transformations of spatial correlation lengths in random fields. *Computers and Geotechnics*, *136*, 104151. https://doi.org/10.1016/j.compgeo.2021.104151

Puła, W., & Zaskórski, Ł. (2015). On Some Methods in Safety Evaluation in Geotechnics. *Studia Geotechnica et Mechanica*, *37*(2), 17–32. https://doi.org/10.1515/sgem-2015-0016

Rezaie Soufi, G., Jamshidi Chenari, R., & Karimpour Fard, M. (2020). Influence of random heterogeneity of the friction angle on bearing capacity factor Nγ. *Georisk*, *14*(1), 69–89. https://doi.org/10.1080/17499518.2019.1566554

Schultze, E., & Menzenbach, E. (1961). Standard penetration test and compressibility of soils. *Proceedings of the Fifth International Conference on Soil Mechanics and Foundation Engineering*, *1*, 527–532.

Selmi, M., Kormi, T., Hentati, A., & Bel Hadj Ali, N. (2019). Capacity assessment of offshore skirted foundations under HM combined loading using RFEM. *Computers and Geotechnics*, *114*, 103148. https://doi.org/10.1016/j.compgeo.2019.103148

Shu, S., Gao, Y., Wu, Y., Ye, Z., & Song, S. (2020). Bearing capacity and reliability analysis of spudcan foundations embedded at various depths based on the non-stationary random finite element method. *Applied Ocean Research*, *100*, 102182. https://doi.org/10.1016/j.apor.2020.102182

Smith, I. M., Griffiths, D. V., & Margetts, L. (2013). *Programming the finite element method*. John Wiley & Sons.

Som, M. N., & Das, S. C. (2003). *Theory and practice of foundation design*. PHI Learning Pvt. Ltd.

Tan, X., Hu, X., & Wu, K. (2009). Fuzzy random finite element reliability analysis of slope stability with fuzzy basic veriables and fuzzy states. *Yanshilixue Yu Gongcheng Xuebao/Chinese Journal of Rock Mechanics and Engineering*, *28*(SUPPL. 2), 3952–3958.

Terzaghi Karl. (1943). *Theoretical soil mechanics. New York: John Wiley & Sons*.

Viviescas, J. C., Mattos, Á. J., & Osorio, J. P. (2021). Uncertainty quantification in the bearing capacity estimation for shallow foundations in sandy soils. *Georisk*, *15*(3), 182–195. https://doi.org/10.1080/17499518.2020.1753782

Zhang, Q. L., & Peil, U. (1997). Random finite element analysis for stochastical responses of structures. *Computers and Structures*, *62*(4), 611–616. https://doi.org/10.1016/S0045-7949(96)00246-5

Zienkiewicz, O. C., & Cormeau, I. C. (1974). Visco-plasticity—plasticity and creep in elastic solids—a unified numerical solution approach. *International Journal for Numerical Methods in Engineering*, *8*(4), 821–845.

Zienkiewicz, O. C., Humpheson, C., & Lewis, R. W. (1977). Associated and non-associated visco-plasticity and plasticity in soil mechanics. *Geotechnique*, *27*(1), 101–102. https://doi.org/10.1680/geot.1977.27.1.101

Zienkiewicz, O. C., Valliappan, S., & King, I. P. (1969). Elasto-plastic solutions of engineering problems 'initial stress', finite element approach. *International Journal for Numerical Methods in Engineering*, *1*(1), 75–100.